Proceedings of the 2006 American Control Conference
Minneapolis, Minnesota, USA, June 14-16, 2006

Performance of Variable-gain Controlled Optical Storage Drives

Marcel Heertjes
Philips Applied Technologies
High Tech Campus 7
Eindhoven, The Netherlands
marcel.heertjes@philips.com

Nathan van de Wouw
Eindhoven University of Techn.
Dept. of Mechanical Engineering
Eindhoven, The Netherlands
n.v.d.wouw@tue.nl

Erik Pastink
Océ Technologies
Venlo, The Netherlands
erik.pastink@oce.nl

Alexey Pavlov
NTNU
Dept. of Engineering Cybern.
Trondheim, Norway
alexey.pavlov@itk.ntnu.no

Henk Nijmeijer
Eindhoven University of Techn.
Dept. of Mechanical Engineering
Eindhoven, The Netherlands
h.nijmeijer@tue.nl

Maarten Steinbuch
Eindhoven University of Techn.
Dept. of Mechanical Engineering
Eindhoven, The Netherlands
m.steinbuch@tue.nl

***Abstract*— A method for performance assessment of a variable-gain control design for optical storage drives is proposed based on a quantitative performance measure. The variable-gain strategy is used to overcome well-known control design tradeoffs (for linear systems) between low-frequency tracking properties and high-frequency noise sensitivity. A performance analysis is conducted to support the design of the variable-gain controller which subsequently is shown to outperform linear controllers.**

I. INTRODUCTION

Optical storage drives such as CD or DVD drives are generally controlled using linear (PID-type) control strategies. For portable or automotive applications, the requirements on the control design relate to both tracking requirements and disturbance attenuation properties. Herein two types of disturbances can be distinguished: low-frequent shock disturbances due to engine vibration or road excitation (shocks), and high-frequent disturbances induced by corruption of the servo position measurement by finger prints, scratches and dirt spots on the disc (disc defects).

Under linear control, the following design trade-off is inherently present: increasing the closed-loop bandwidth improves the low-frequency disturbance rejection properties under shocks and vibrations at the cost of deteriorating the sensitivity to high-frequency measurement noise in the presence of disc defects [2]. Nonlinear control, or more specifically, nonlinear PID control, see also [1] and the references therein, combines the possibility of having increased performance in terms of shock attenuation without unnecessarily deteriorating the time response under disc defect disturbances. In [4], variable-gain control strategies are proposed to overcome the practical implications of such design limitations. Often, however, the comparison between control designs is based on time- and frequency-domain simulations and experiments and, therefore, does not directly support a quantitative comparison of the performance of different nonlinear and linear controllers.

In this paper, we propose a performance measure and will use it to support a performance-based control design for variable-gain controlled optical storage drives. We design the controller such that the closed-loop system is convergent, [6], which implies asymptotic stability of the unperturbed system and the existence of a unique bounded periodic steady-state solution for every harmonic disturbance. We adopt the perspective of exactly computing the steady-state responses (which are unique by virtue of the convergence property) to disturbances from the specific class of harmonic disturbances and defining the control performance on the basis of these quantitative data. Performance in the face of harmonic disturbances is specifically important for optical storage drives since in practice the performance is tested experimentally by constructing so-called 'Drop-Out-Level Curves' [3], which show the level of the harmonic disturbance for which a termination of the disc read-out occurs for varying disturbance frequencies.

The remainder of this paper is organized as follows. In section II, a simplified model of the storage drive dynamics (in radial direction) is given along with the variable-gain control strategy. Section III introduces the class of convergent systems and proposes the conditions for convergence. In section IV, the performance measure is introduced and used to discriminate between different control designs. The main conclusions are summarized in section V.

II. STORAGE DRIVE MODELLING

A simplified model for the lens actuator dynamics of an optical storage drive in so-called radial direction is depicted schematically in Figure 1. Herein, r reflects a combination of signals such as the reference position of the track to be read and its possible corruption due to disc vibrations. The two-stage control strategy of the optical pick-up unit consists of a long-stroke motion of a sledge containing the lens (p_{ls}) and a short-stroke motion of the lens with respect to the sledge (p_{ss}). We primarily focus on the control of the short-stroke motion (i.e. p_{ls} is assumed fixed). The lens dynamics in the sledge are modelled by a mass-spring-damper system with mass m, stiffness k and damping b.

1-4244-0210-7/06/$20.00 ©2006 IEEE

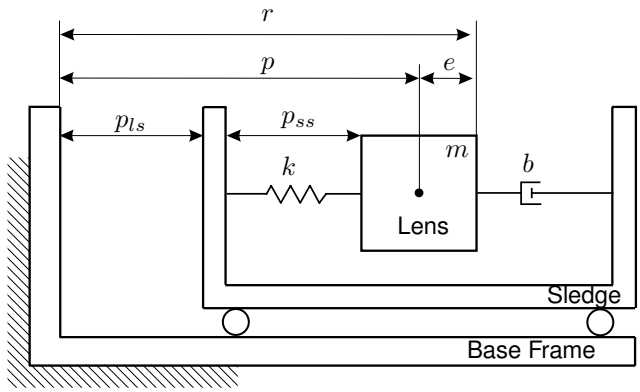

Fig. 1. Model of the lens actuator dynamics.

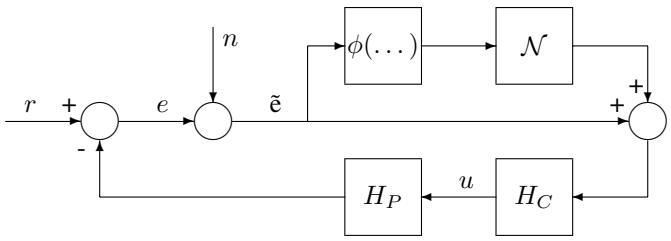

Fig. 2. Block diagram of a variable-gain controlled optical storage drive.

A block-diagram of the controlled lens dynamics is given in Figure 2. Herein, n represents measurement noise and u is the control action. It should be noted that in optical storage drives the error e (of the lens with respect to the disc track) is the measured variable. Since this signal generally is corrupted by measurement noise it is denoted by $\tilde{e}$. Moreover, $H_P(s)$ represents the transfer function (in the Laplace domain) related to the lens (and actuator) dynamics:

$$H_P(s) = \frac{1}{ms^2 + bs + k}\,\frac{\omega_a}{s + \omega_a}, \quad s \in \mathbb{C}, \tag{1}$$

with ω_a the breakpoint of a low-pass filter, which is due to the actuator inductance from voltage to current. The transfer function $H_C(s)$ representing the PID-controller including a second-order low-pass filter is given by

$$H_C(s) = k_p \frac{\omega_{lp}^2\left(s^2 + (\omega_d + \omega_i)s + \omega_d\omega_i\right)}{\omega_d\left(s^3 + 2\beta\omega_{lp}s^2 + \omega_{lp}^2 s\right)}, \quad s \in \mathbb{C}, \tag{2}$$

where ω_i is the breakpoint of the integral action, ω_d is the breakpoint of the differential action, ω_{lp} and β denote the breakpoint and the damping parameter of the low-pass filter, respectively, and k_p is the loop gain.

The basic idea behind the variable-gain control design is that, firstly, when the error is small a low-gain design should be in effect to ensure low sensitivity to high-frequency measurement noise and, secondly, when the error becomes large due to low-frequency shocks a high-gain design should be active to ensure a high level of low-frequency tracking performance. In Figure 2, the variable gain strategy is realized through the addition of the variable-gain element $\phi(\tilde{e})$:

$$\phi(\tilde{e}) = \begin{cases} \alpha - \frac{\alpha\delta}{|\tilde{e}|} & \text{if } |\,\tilde{e}\,| \geq \delta \\ 0 & \text{if } |\,\tilde{e}\,| < \delta \end{cases}. \tag{3}$$

The parameters $\alpha \geq 0$ and $\delta \geq 0$ represent the additional gain and the dead zone length, respectively. Hence within the dead-zone ($|\tilde{e}| < \delta$) the low-gain design is effective and outside the dead-zone an additional gain $\phi(\tilde{e})$ is applied.

To enhance the shock suppression properties via large additional gains, such as studied in [3], the usage of the variable gain element $\phi(\tilde{e})$ (referred to as the static nonlinear case) is compared with the situation where a dynamic filter $\mathcal{N}$ is added in the nonlinear feedback path, see Figure 2. The latter being referred to as the dynamic back-end nonlinear case. The filter $\mathcal{N}$ is given by

$$\mathcal{N}(s) = n_1\omega_{lpf}\frac{s^2 + 2\zeta_1 s + \omega_{f1}^2}{(s^2 + 2\zeta_2 s + \omega_{f2}^2)(s + \omega_{lpf})}, \tag{4}$$

with ω_{f1} and ω_{f2} notch breakpoints, ζ_1 and ζ_2 the notch damping coefficients, ω_{lpf} the breakpoint of a first-order low-pass filter, and n_1 a scaling factor.

For the purpose of stability analysis, a state-space notation will be adopted, which is given by

$$\begin{aligned} \dot{x} &= Ax + B\gamma(\tilde{e}) + B[\underbrace{r(t) + n(t)}_{q(t)}] \\ \tilde{e} &= \underbrace{r(t) + n(t)}_{q(t)} - Cx, \end{aligned} \tag{5}$$

with the state vector $x \in \mathbb{R}^9$, the measured radial error signal $\tilde{e} \in \mathbb{R}$ and the scalar nonlinearity $\gamma(\tilde{e}) = \phi(\tilde{e})\tilde{e}$ due to the variable-gain element.

In stability analysis of the closed-loop system we are now interested in the following question: under what conditions of the controller parameters do all solutions of the closed-loop system (5) corresponding to a bounded input signal $q(t)$ converge to a unique bounded steady-state solution? This property of the closed-loop system – the so-called convergence property – as well as an answer to the above stated question are discussed in the next section.

III. CONVERGENT SYSTEMS

A system is called convergent if for any bounded input $w(t)$ all its solutions converge to some bounded steady-state solution $\bar{x}_w(t)$ which is determined only by the input $w(t)$, see [6]. Such systems have an additional property that if the input $w(t)$ is constant, the corresponding steady-state solution is also constant. If, however, the input $w(t)$ is periodic with period T, then the corresponding steady-state solution $\bar{x}_w(t)$ is also periodic with the same period T. For systems of the form

$$\begin{aligned} \dot{x} &= Ax + B\sigma(y) + w_1(t) \\ y &= w_2(t) - Cx, \end{aligned} \tag{6}$$

(note that this form conforms with (5)) with state $x \in \mathbb{R}^n$, input $w = [w_1^T, w_2]^T \in \mathbb{R}^{n+1}$ and scalar nonlinearity $\sigma(y)$

depending on the scalar output y, exponential convergence (see [7]) can be verified with the following result.

Theorem 1: Consider system (6). Suppose the matrix A is Hurwitz and the nonlinearity $\sigma(y)$ satisfies the incremental sector condition

$$0 \leq \frac{\sigma(y_1) - \sigma(y_2)}{y_1 - y_2} \leq \mu \, , \, \forall \, y_1, y_2 \in \mathbb{R} \mid y_1 - y_2 \neq 0, \quad (7)$$

where $\mu \in [0 \, , \, \infty)$. If the system satisfies the condition

$$\Re \{G(j\omega - \lambda)\} > -\frac{1}{\mu} \, , \, \forall \, \omega \in \mathbb{R}, \quad (8)$$

for some $\lambda \geq 0$, where $G(s) := C(sI - A)^{-1}B$, then system (6) is exponentially convergent for any bounded piecewise-continuous input $w(t)$. Moreover, the steady-state solution is globally exponentially stable with an exponent $\tilde{\lambda}$ satisfying $\tilde{\lambda} > \lambda$, i.e. it holds that

$$\| \, \bar{x}_w(t) - x(t) \, \| \leq \beta e^{-\tilde{\lambda}(t-t_0)} \, \| \, \bar{x}_w(t_0) - x(t_0) \, \| \, , \, \forall \, t > t_0, \quad (9)$$

for some $\beta > 0$ independent of the particular input $w(t)$.

Proof: For the case that $w_2(t) \equiv 0$ this theorem was proved in [9]. For the case that $w_2(t) \not\equiv 0$, notice that for all $x_1, x_2 \in \mathbb{R}^n$ such that $Cx_1 - Cx_2 \neq 0$ the time-varying nonlinearity $\sigma(w_2(t) - Cx)$ satisfies

$$\begin{aligned} &\frac{\sigma(w_2(t) - Cx_1) - \sigma(w_2(t) - Cx_2)}{-Cx_1 + Cx_2} \\ &= \frac{\sigma(w_2(t) - Cx_1) - \sigma(w_2(t) - Cx_2)}{(w_2(t) - Cx_1) - (w_2(t) - Cx_2)}. \end{aligned} \quad (10)$$

Therefore, by condition (7) we obtain

$$\begin{aligned} 0 \leq &\frac{\sigma(w_2(t) - Cx_1) - \sigma(w_2(t) - Cx_2)}{-Cx_1 + Cx_2} \leq \mu \\ &\forall \, t \in \mathbb{R}, x_1, x_2 \in \mathbb{R}^n \mid Cx_1 - Cx_2 \neq 0. \end{aligned} \quad (11)$$

Once condition (11) is established, the proof of exponential convergence and inequality (9) repeats the proof from [9] for the case of $w_2(t) \equiv 0$.□

Note that the closed-loop system (5) is in the form (6) with $y = \tilde{e}$, $\sigma(y) = \gamma(\tilde{e})$, $w_1(t) = Bq(t)$ and $w_2(t) = q(t)$. Furthermore, it can be verified that the nonlinearity γ satisfies the incremental sector condition (7) with $\alpha \in [0 \, , \, \infty)$ representing the additional gain. Besides, we assume the system matrix A to be Hurwitz. In order to guarantee exponential convergence, we require that system (5) satisfies (8) for $\mu = \alpha$, some $\lambda \geq 0$, and given the matrices A, B and C. This allows for a graphical study.

The left part of Figure 3 displays the Nyquist plot of $G(j\omega - \lambda)$ for $\lambda = 10$ ($\mathcal{N} = 1$). Condition (8) is satisfied if the Nyquist plot of $G(j\omega - \lambda)$ is entirely on the right side of the line l vertically passing through $-\frac{1}{\alpha}$. Hence, α can be increased up to the value at which l is just tangent to the Nyquist plot of $G(j\omega - \lambda)$. For system (5), in case $\lambda = 10$, α is restricted to a maximum value of 1.82. The frequency-domain condition (8) is fulfilled for various combinations of α and λ. The right part of Figure 3 depicts a curve in the (α, λ) space, which establishes what *minimum* value of λ can be assured if condition (8) is satisfied, given a particular

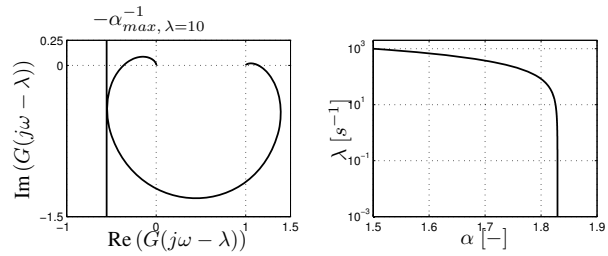

Fig. 3. Left: Nyquist plot of $G(j\omega - \lambda)$ for $\lambda = 10$, and graphical investigation of frequency-domain condition (8). Right: Relation between α and the minimum level of λ when condition (8) is satisfied.

value of α. The latter curve indicates a stability region just like the Nyquist plot in the left part of Figure 3. Namely, for all α on the left side of the vertical asymptote at $\alpha \approx 1.82$, condition (8) is satisfied. Generally, this asymptote can be extended to much larger values ($\alpha \approx 11.4$) by introducing dynamic filtering ($\mathcal{N} = \mathcal{N}(j\omega)$) such as shown in [3]. This gives the possibility of having improved shock suppression.

IV. PERFORMANCE ASSESSMENT

In this section, we consider disturbance modelling, provide a quantitative performance measure, and discuss its usage in variable-gain control systems tuning.

A. DISTURBANCE MODELLING

At this point, we revert to the notation introduced in section II: r represents disc vibrations and n denotes the measurement noise. Once more, the perspective of harmonic disturbances is taken:

$$\begin{aligned} r(t,\Omega_r, Q_r) &= Q_r \, |F_r(j\Omega_r)| \sin(\Omega_r t) \\ &\forall \, t \in \mathbb{R} \, , \, \forall \, \Omega_r \times Q_r \in [\Omega_r^- \, , \, \Omega_r^+] \times [Q_r^- \, , \, Q_r^+], \end{aligned} \quad (12)$$

and

$$\begin{aligned} n(t,\Omega_n, Q_n) &= Q_n \, |F_n(j\Omega_n)| \sin(\Omega_n t) \\ &\forall \, t \in \mathbb{R} \, , \, \forall \, \Omega_n \times Q_n \in [\Omega_n^- \, , \, \Omega_n^+] \times [Q_n^- \, , \, Q_n^+], \end{aligned} \quad (13)$$

where Q_r and Q_n represent the amplitudes of the disc vibrations r and the measurement noise n, respectively. Similarly, Ω_r and Ω_n represent the frequencies of the disc vibrations r and the measurement noise n, respectively. The linear filters $F_r(j\Omega_r)$ and $F_n(j\Omega_n)$ enable appropriate frequency weighting. The introduced notation expresses the fact that disc vibrations are only considered in the frequency range $[\Omega_r^-, \Omega_r^+]$ and an amplitude range $[Q_r^-, Q_r^+]$. Similarly, measurement noise is only considered in the frequency range $[\Omega_n^- \, , \, \Omega_n^+]$ and an amplitude range $[Q_n^- \, , \, Q_n^+]$.

By the notation $e(t, \Omega, Q)$ and $p(t, \Omega, Q)$ we indicate the error response and the displacement of the lens to a harmonic disturbance with amplitude Q and angular frequency Ω, respectively. Moreover, by $||e(t, \Omega, Q)||_\infty = \sup_{t \in [0,T]} \{|e(r(t, \Omega, Q))|\}$, with $T = (2\pi)/\Omega$ being the period time of the disturbance, we denote the maximum absolute error occurring on the periodic steady-state solution induced by the periodic disturbance.

According to the Drop-Out-Level curve [3], the spectral contents of radial disc displacements is in the range from 10 to 200 Hz. Therefore, we set $[\Omega_r^-\ ,\ \Omega_r^+] = [10\cdot 2\pi\ ,\ 200\cdot 2\pi]$ rad/s. The maximum amplitude of the disc vibrations Q_r^+ and the filter $F_r(j\Omega_r)$ are chosen such that the combination induces the occurrence of a terminated disc readout (commonly called a mute). The occurrence of a mute conforms to the maximum radial error level in optical disc drives. Namely if the error exceeds a quarter of the track pitch, which for the exemplary case of CD yields $\|e(r(t,\Omega_r,Q_r))\|_\infty > 4\cdot 10^{-7}$ m, the lens can loose the current track. Now, we choose the filter $F_r(j\Omega_r)$ such that for a maximal disc vibration amplitude of $Q_r^+ = 4\cdot 10^{-7}$ m, the disc readout is terminated for all disturbance frequencies when the low-gain control design is implemented. For the low-gain linear design (the design with $\alpha = 0$), $\|e(r(t,\Omega_r,Q_r))\|_\infty$ is related to the disturbance through the low-gain sensitivity function $S_{lg}(j\omega)$:

$$\begin{aligned}\|e(r(t,\Omega_r,Q_r))\|_\infty &= \left\|\mathcal{F}^{-1}\left\{S_{lg}(j\omega)R(j\omega,\Omega_r,Q_r)\right\}\right\|_\infty \\ &= Q_r\left|S_{lg}(j\Omega_r)F_r(j\Omega_r)\right|,\end{aligned} \tag{14}$$

where $R(j\omega,\Omega_r,Q_r) = \mathcal{F}\{r(t,\Omega_r,Q_r)\}$ is the Fourier transform of $r(t,\Omega_r,Q_r)$. By choosing $|F_r(j\Omega_r)| = \left|S_{lg}^{-1}(j\Omega_r)\right|$, $\forall\ \Omega_r \in [10\cdot 2\pi\ ,\ 200\cdot 2\pi]$, we guarantee that the disc readout is terminated for $Q_r = Q_r^+$, $\forall \Omega_r \in [10\cdot 2\pi\ ,\ 200\cdot 2\pi]$. Note that $\left|S_{lg}^{-1}(j\Omega_r)\right|$ has a low-pass characteristic for $\Omega_r \in [10\cdot 2\pi\ ,\ 200\cdot 2\pi]$, see the left part of Figure 4.

By assuming that the frequency contents of measurement noise due to disc defects starts at 3 kHz [1], see [8], [5], we set $\Omega_n^- = 3\cdot 10^3\cdot 2\pi$ rad/s. Furthermore, the highest frequency at which measurement noise can possibly disturb the output is dictated by half the sample frequency which amounts 45 kHz [2]. Consequently, we define $\Omega_n^+ = 4.5\cdot 10^4\cdot 2\pi$ rad/s. The transfer function from measurement noise to the measured radial error is given by the sensitivity function. Using this fact, it is obtained that

$$\begin{aligned}\|\tilde{e}(n(t,\Omega_n,Q_n))\|_\infty &= \left\|\mathcal{F}^{-1}\left\{S_{lg}(j\omega)N(j\omega,\Omega_n,Q_n)\right\}\right\|_\infty \\ &= Q_n\left|S_{lg}(j\Omega_n)F_n(j\Omega_n)\right|,\end{aligned} \tag{15}$$

where $N(j\omega,\Omega_n,Q_n) = \mathcal{F}\{n(t,\Omega_n,Q_n)\}$ is the Fourier transform of $n(t,\Omega_n,Q_n)$. To respect the maximum level of $\tilde{e}$ experienced in practice, Q_n^+ is upper bounded through $Q_n^+\left|S_{lg}(j\Omega_n)F_n(j\Omega_n)\right| = 10^{-7}$, $\Omega_n \in [3\cdot 10^3\cdot 2\pi, 4.5\cdot 10^4\cdot 2\pi]$ which is guaranteed if we set $Q_n^+ = 10^{-7}$ m and define $|F_n(j\Omega_n)| = \left|S_{lg}^{-1}(j\Omega_n)\right|$, $\forall \Omega_n \in [3\cdot 10^3\cdot 2\pi, 4.5\cdot 10^4\cdot 2\pi]$, see the right part of Figure 4. Note that $[\Omega_r^-\ ,\ \Omega_r^+]\bigcap[\Omega_n^-\ ,\ \Omega_n^+] = \emptyset$, which avoids conflicting goals otherwise encountered when both disturbances show an overlap in frequency range.

[1]At a rotation speed of 10 Hz and at a radius of 0.04 m, an 800 μm black dot needs approximately $\{3\text{ kHZ }\}^{-1}$ to pass.

[2]The upper bound of 45 kHz is a control design limitation due to finite sampling frequency rather than a characterization of disc defects.

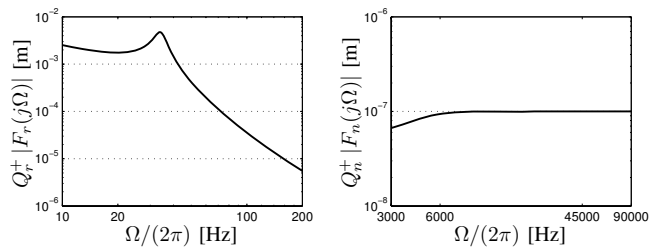

Fig. 4. Design weighting filters and maximum levels of disturbance as a function of frequency.

B. Performance Measure

Given $[\Omega_r^-\ ,\ \Omega_r^+]\bigcap[\Omega_n^-\ ,\ \Omega_n^+] = \emptyset$, the performance measure P – an integral deviation formulation – is given by:

$$P = \frac{\displaystyle\int_{Q_r^-}^{Q_r^+}\int_{\Omega_r^-}^{\Omega_r^+}\|e(r(t,\Omega_r,Q_r))\|_\infty\, d\Omega_r dQ_r + \ldots}{\displaystyle\int_{Q_r^-}^{Q_r^+}\int_{\Omega_r^-}^{\Omega_r^+}\|e_{ref}(r(t,\Omega_r,Q_r))\|_\infty\, d\Omega_r dQ_r + \ldots}\ \frac{\displaystyle\ldots\int_{Q_n^-}^{Q_n^+}\int_{\Omega_n^-}^{\Omega_n^+}\|y(n(t,\Omega_n,Q_n))\|_\infty\, d\Omega_n dQ_n}{\displaystyle\ldots\int_{Q_n^-}^{Q_n^+}\int_{\Omega_n^-}^{\Omega_n^+}\|y_{ref}(n(t,\Omega_n,Q_n))\|_\infty\, d\Omega_n dQ_n}, \tag{16}$$

where $\bar{Q} \subseteq \mathbb{R}^+$ and $\bar{\Omega} \subseteq \mathbb{R}^+$. The first integral in (16), i.e. the integral over $\bar{Q}$, accounts for the conceivable amplitude dependency inherent to the variable-gain control design. The second integral, i.e. the integral over Ω, accounts for the frequency dependency of the closed-loop behavior. Note that in defining (16), it is presumed that the integrands are integrable with respect to Ω and Q, a fact which results from the convergence properties of the closed-loop system. The response of an arbitrary reference design is indicated by means of the subscript *ref* in the denominator of (16). The integral deviation formulation is defined as a relative measure to facilitate the interpretation of its outcome. Hence, the denominator in (16) is merely included for scaling purposes. If the control design under evaluation (related to the numerator of (16)) and the reference design yield equal performance, a value $P = 1$ is obtained. If, however, $P < 1$, the control design under evaluation yields a better performance than its reference design; in the remainder of this paper the low-gain linear design is chosen to serve as the reference design.

C. Performance-based control design

To illuminate qualitative contributions of improvement/deterioration with respect to low-frequency disturbance rejection and high-frequency measurement noise sensitivity to the performance P, a two-part separation of the nominator in (16) can be motivated as follows. Provided Ω_r^+ is below the bandwidth of the reference design, through the first part

(referred to as P_r) the conceivable improvement in low-frequency disturbance rejection is studied. Furthermore, provided that Ω_n^- is above the bandwidth of the reference design, the second part (referred to as P_n) enables a quantification of the possible deterioration of measurement noise sensitivity. The dimensionless interpretation of P applies to both parts as well, that is: (i) if $P_r < 1$ an improvement in low-frequency disturbance rejection is obtained, (ii) if $P_n > 1$ a worsening of performance (here performance reflects the lack of sensitivity to measurement noise) is acquired, and viceversa.

For the static nonlinear case ($\mathcal{N}(s) = 1$), Figure 5 depicts the outcome of (16) as a function of α evaluated for the disturbances defined in Section IV-A. Furthermore, P is evaluated for several levels of the dead-zone length δ. The figure indicates that the performance depends strongly on both α and δ. For all levels of δ, it is obtained that $P \to 1$ if $\alpha \downarrow 0$ because the reference design and the variable gain control design under evaluation are equal in this particular case. If $\delta \geq 4{\cdot}10^{-7}$ m, it is obtained that $P = 1 \forall \alpha \in [0, 1.82]$. The reason for this fact is twofold. If $\delta \geq 4{\cdot}10^{-7}$ m the dead-zone will not be exceeded because (i) the error due to radial disc displacements is upper-bounded by $4 \cdot 10^{-7}$ m, and (ii) the measured radial error resulting from measurement noise is upper-bounded by 10^{-7} m.

Initially, a reduction of δ will enhance performance because low-frequency disturbance rejection properties are improved whereas the measurement noise sensitivity remains unaltered, see the curves for $\delta \in \{3 \cdot 10^{-7}, 2 \cdot 10^{-7}, 10^{-7}\}$ m. For these levels of δ, P decreases monotonically with α and therefore maximum performance, i.e. minimum P, is obtained if $\alpha = 1.82$.

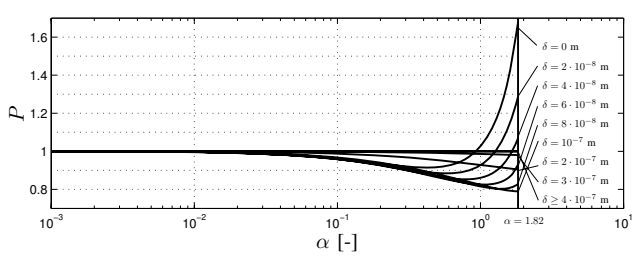

Fig. 5. P for the static nonlinear case.

A further decrease of δ results in a deterioration of performance compared to the design with $\delta = 10^{-7}$ m. Namely, if $\delta < 10^{-7}$ m, the measured radial error resulting from measurement noise will exceed the dead-zone length and hence, a deterioration of the measurement noise sensitivity is effected. Consequently, P no longer monotonically decreases with α and therefore, maximum performance is no longer obtained for maximum α.

If $\delta \in \{8{\cdot}10^{-8}, 6{\cdot}10^{-8}\}$ m, the variable gain control design under evaluation still accomplishes better performance than the reference design for all $\alpha \in [0\ ,\ 1.82]$. However, for $\delta \in \{4{\cdot}10^{-8}, 2{\cdot}10^{-8}, 0\}$ m there exist values for α for which $P > 1$, implying a deterioration of the performance compared to the low-gain linear design. Here, the improvement in low-frequency disturbance rejection properties is cancelled by the deterioration of the measurement noise sensitivity. Therefore, for smaller levels of δ, the increase of the gain α within the range for which convergence is guaranteed, does not lead to an improved performance.

Depending on the combination of α and δ, the variable gain control design can outperform both the low-gain and the high-gain linear design (with $\phi(\tilde{e}) = \alpha$). That is, given the performance measure (16), the weighting filters in Figure 4 and the disturbance modelling proposed in section IV-A, Figure 5 clearly shows that nonlinear control can prevail over linear control.

For the dynamic back-end nonlinear case (with $\mathcal{N}$ given by (4)), Figure 6 shows performance with respect to the static

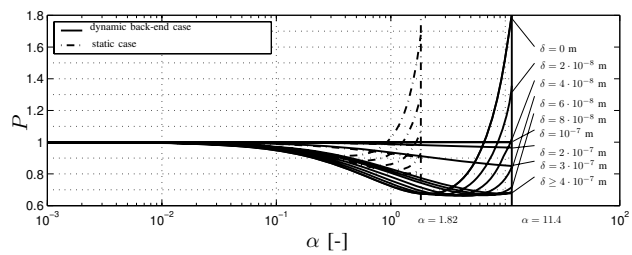

Fig. 6. P for the dynamic back-end nonlinear case.

nonlinear cases. Although barely visible, for $\alpha \in [0\ ,\ 1.82]$ and $\delta \in \{3{\cdot}10^{-7}, 2{\cdot}10^{-7}, 10^{-7}\}$, the system supplied with the static nonlinearity outperforms the back-end dynamic nonlinearity case. For these levels of δ, a monotonic decrease of P with α is obtained. That is, minimum P, hence maximum performance, is obtained at $\alpha = 11.4$, *i.e.*, a level that can merely be obtained by the aid of $\mathcal{N}$. This gives the motivation from a performance point of view to include $\mathcal{N}$. For $\alpha \in [0\ ,\ 1.82]$ and $\delta < 10^{-7}$, the system supplied with the dynamic back-end nonlinearity enables significantly better performance than for the static nonlinear case. If $\delta > 10^{-7}$, maximum performance is no longer obtained for maximum α. None the less, it can be seen that apart from $\delta \in \{2{\cdot}10^{-8}, 0\}$, the dynamic back-end nonlinear case induces smaller P hence better performance than its linear equivalent.

V. CONCLUSIONS

The contribution of this paper lies in the following aspects. Firstly, a convergence-based control design is proposed, which guarantees stability of the closed-loop system and a unique bounded steady-state response for any bounded disturbance. Secondly, a quantitative performance measure, taking into account both low-frequency tracking properties and high-frequency measurement noise sensitivity, is proposed to support the design and tuning of the nonlinear (non-smooth) control design. The proposed performance measure is based on the computed steady-state responses to a class of harmonic disturbances. Such a measure is consistent with industrial performance specifications. The convergence conditions together with the performance measure jointly constitute a design tool for tuning the parameters of the

variable-gain controller which is shown to outperform the underlying linear control designs.

REFERENCES

[1] B. Armstrong, D. Neevel, and Kusid T. New results in NPID control: tracking, integral control, friction compensation and experimental results. *IEEE Transactions on Control Systems Technology*, 9(2):399–406, 2001.

[2] J. Freudenberg, Middleton R., and A. Stefanopoulou. A survey of inherent design limitations. In *Proceedings of the American Control Conference*, pages 2987–3001, Chicago, Illinois, USA, 2000.

[3] M.F. Heertjes, F. Cremers, M. Rieck, and M. Steinbuch. Nonlinear control of optical storage drives with improved shock performance. *Control Engineering Practice*, 13(10):1295–1305, 2005.

[4] M.F. Heertjes, H.A. Pastink, N. van de Wouw, and H. Nijmeijer. Experimental frequency-domain analysis of nonlinear controlled optical storage drives. *IEEE Transactions on Control Systems Technology*, 2005. Accepted.

[5] J. Helvoirt, G.A.L. Leenknegt, M. Steinbuch, and H.J. Goossens. Classifying disc defects in optical disc drives by using time-series clustering. In *Proceedings of the American Control Conference*, pages 3100–3105, Boston, Massachusetts, USA, 2004.

[6] A. Pavlov, N. van de Wouw, and H. Nijmeijer. Convergent systems: analysis and design. In T. Meurer, K. Graichen, and D.Gilles, editors, *Control and Observer Design for Nonlinear Finite and Infinite Dimensional Systems. Lecture Notes in Control and Information Sciences, vol. 322*. 2005.

[7] A.V. Pavlov. *The output regulation problem: a convergent dynamics approach*. PhD thesis, Eindhoven University of Technology, Eindhoven, 2004.

[8] E. Vidal, P. Andersen, J. Stoustrup, and T.S. Pedersen. A study on the surface defects of a compact disk. In *Proceedings of the IEEE Conference on Control Applications*, pages 101–104, Mexico City, Mexico, 2001.

[9] V.A. Yakubovich. The matrix inequality method in the theory of the stability of nonlinear control systems - i. the absolute stability of forced vibrations. *Automation and remote control*, 7:905–917, 1964.